



ELSEVIER

Available online at [www.sciencedirect.com](http://www.sciencedirect.com)

SCIENCE @ DIRECT®

PHOTONICS AND  
NANOSTRUCTURES  
Fundamentals and Applications

Photonics and Nanostructures – Fundamentals and Applications xxx (2003) xxx–xxx

[www.elsevier.com/locate/photronics](http://www.elsevier.com/locate/photronics)

## Optical properties of a three-dimensional silicon square spiral photonic crystal

Scott R. Kennedy<sup>a,\*</sup>, Michael J. Brett<sup>a</sup>, Hernan Miguez<sup>b</sup>,  
Ovidiu Toader<sup>c</sup>, Sajeev John<sup>c</sup>

<sup>a</sup> Department of Electrical and Computer Engineering, University of Alberta, Edmonton, AB, Canada T6G 2V4

<sup>b</sup> Fibre Radio Group, Instituto de Investigación ITACA, Universidad Politécnica de Valencia, 46020 Valencia, Spain

<sup>c</sup> Department of Physics, University of Toronto, Toronto, Ont., Canada M5S 1A7

Received 30 May 2003; received in revised form 30 May 2003; accepted 4 June 2003

### Abstract

We report the fabrication and optical characterization of a tetragonal square spiral photonic crystal with a three-dimensional relative band gap of approximately 10% using the glancing angle deposition (GLAD) technique. This thin film structure is produced in a one-step process that is highly versatile as a wide range of crystal structures can be created simply through the variation of deposition parameters. Measurements indicate upper and lower frequency band edges at vacuum wavelengths of 2.50 and 2.75  $\mu\text{m}$ , in the infrared region of the spectrum.

© 2003 Elsevier B.V. All rights reserved.

PACS: 42.70.Qs; 81.15.Tv

**Keywords:** Thin film; Photonic crystal; Photonic band gap; Fabrication

Photonic band gap (PBG) crystals are complex structures of periodically alternating materials with the ability to localize light of wavelengths comparable to the periodicity of the lattice [1,2]. Microscopic scattering and macroscopic Bragg resonances for frequencies of light falling within the PBG of the structure are responsible for this phenomenon that is analogous to electron localization in the periodic potential of a semiconductor crystal lattice. Within the characteristic band gap, incident light is pro-

hibited from propagating, a feature that is of great importance in applications of both active and passive micro-photonic devices. However, because of the complexity of the periodic structure that must be arranged on a sub-micron scale, fabrication of PBG crystals is traditionally difficult and requires careful control of processes such as self-assembly [3] or complex lithography and/or etching [4,5]. Here, we demonstrate a three-dimensional (3D) photonic crystal fabricated by a unique thin film deposition technique, glancing angle deposition (GLAD), that is highly versatile and can virtually reduce the fabrication of large gap PBG crystals to a single step.

\* Corresponding author. Tel.: +780-492-7926;

fax: +780-492-2863.

E-mail address: [skennedy@ee.ualberta.ca](mailto:skennedy@ee.ualberta.ca) (S.R. Kennedy).

Toader and John originally proposed the tetragonal square spiral structure [6] as a promising candidate for large gap photonic crystals, due to its potential ease of fabrication. Unlike earlier circular spiral lattices proposed by Chutinan and Noda [7], the square spiral lattice requires no phase shift between neighbouring spiral posts. Successful fabrication of the square spiral structure has been reported [8], followed by a more detailed theoretical analysis of the structure and its relationship to the diamond and face-centred-cubic (FCC) lattices with large predicted frequency gaps greater than 16% [9]. Recently, higher-level architectures have also been proposed for integrated optics in an all-optical micro-chip based on the square spiral fabrication process by GLAD [10]. The underlying principle of a square spiral photonic crystal is the interconnection of diamond or FCC lattice points by arms of the film material oriented at right angles to the previous growth direction, where the elbows can also be moved off the diamond points to optimize the PBG. If we define the orientation of the substrate as the [001] plane, and arrange the growth of individual spirals in a tetragonal array, it is possible to connect 1st, 3rd or 5th nearest neighbours of a traditional diamond or FCC lattice by a spiral staircase structure. The resulting crystal can be seen in Fig. 1,

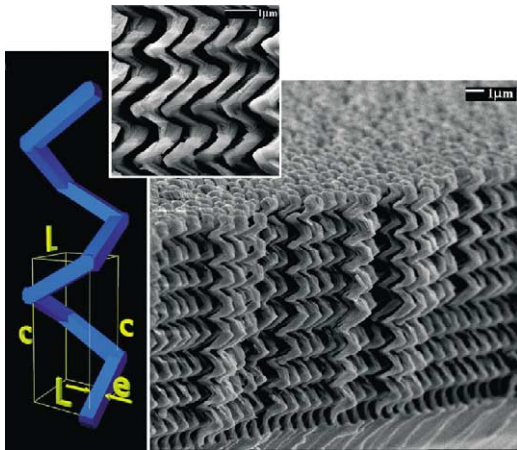


Fig. 1. Oblique and edge view of the tetragonal square spiral photonic crystal with  $[L, c, e] = [0.72, 1.40, 0.37]$  and lattice spacing  $a = 1000$  nm. The film was deposited at  $84^\circ$  from normal and the corners of the square spirals are rotated through  $90^\circ$  with a vertical pitch of 45 nm. The left inset is a single computer-generated square spiral, showing the characteristic parameters of the structure.

where silicon structures have been deposited using GLAD.

The GLAD process is a thin film deposition technique implemented at highly oblique angles of incidence ( $80^\circ$ – $90^\circ$  from normal) to produce porous thin films with unique microstructures [11–13]. Advanced substrate motion is used to control its orientation with respect to the vapour source and provides the film structures with their characteristic shapes. In the production of tetragonal square spiral structures, a pre-seeded substrate that has been patterned by photolithography is used, although many other means of substrate procurement exist [8]. The orientation of the substrate is controlled by a computer and is placed at an oblique angle with a crystal thickness monitor used for deposition rate feedback. On a stationary substrate, slanted posts grow in the relative direction of the vapour source and are isolated from one another due to shadowing effects. The growth locations are initially restricted by the topography of the substrate and subsequently by self-shadowing of the film structures themselves. Square spirals are grown one arm at a time over the entire array of pre-patterned dots, and at intervals characteristic of the desired structure, the substrate is rotated through one-quarter of a turn. Contrary to the previously reported method of fabrication where abrupt  $90^\circ$  turns are executed at regular intervals [8], the crystal structure here has taken advantage of advanced substrate motion and the corners of the square spirals have been improved by the gradual rotation of the substrate through this critical point. In the structure of Fig. 1, the corners are graded with a vertical pitch of 45 nm, i.e. a turn of  $90^\circ$  takes place over vertical film growth of 45 nm. A wide variety of materials may be used with GLAD and as the fabrication of photonic crystals requires large dielectric contrasts, silicon is typically the material of choice.

The silicon square spiral photonic crystal of Fig. 1 was fabricated with a principal lattice constant of  $a = 1000$  nm on a pre-patterned silicon wafer, and from nomenclature developed by two of the authors (O. Toader and S. John) is of the [001]-diamond:1 type [6,9], or 1st nearest neighbour, with  $[L, c, e] = [0.72, 1.40, 0.37]$ . These parameters correspond to a volume-filling factor of solid material of approximately one-third. Eight complete turns of four arms each were grown, resulting in an overall thickness of  $11.2 \mu\text{m}$  and the angle of incidence was held constant

at  $84^\circ$  from normal. The silicon film was deposited by an electron beam source at an ambient system pressure of approximately  $8 \times 10^{-7}$  Torr. The features of the structure were characterized using a JEOL JSM-6301FXV field emission scanning electron microscope and the results used to provide quantitative measurements of the square spiral dimensions.

Previously reported theoretical band structures for square spiral photonic crystals yield a unique band gap between the 4th and 5th band that is very robust [6,8]. As Maxwell's equations for electromagnetic theory are linear, the nomenclature mentioned above represents a gap that is scalable with the lattice parameter,  $a$ . For our film with  $a = 1000$  nm, a centre frequency for the gap is expected at approximately  $2.7 \mu\text{m}$  [9] and for an optimal structure with a 15% relative band gap (for nearest neighbour connection) this would correspond to band edges at  $2.50$  and  $2.90 \mu\text{m}$ . Although the preliminary structure fabricated here is not expected to produce an ideal band gap, these values serve as guides for measurement of the optical properties of the crystal.

In the first set of measurements, a Nicolet Magna-IR 750 Fourier transform infrared (FTIR) spectrometer in reflection mode was used to measure the optical properties of the fabricated crystal. Near-normal incidence reflection measurements were performed to characterize the band properties of the fabricated crystal. The effect of a photonic band gap is the appearance of a large reflectivity plateau over the corresponding range of wavelengths with band edges characterized by transitions from low to high reflection values. In practice, diffuse reflection from minor imperfections and fluctuations in spiral height and cross-section at the photonic crystal surface reduce the detected reflectivity from its ideal value of 100%, inside the PBG, and uncoupled bands may contribute to nonzero reflectivity outside the PBG. Nevertheless, a distinctive reflectivity feature, independent of the incident angle, is expected. The numerical aperture of the source/detector was 0.58 with a half-cone angle of  $35^\circ$ , and the spot size of the optical system was  $250 \mu\text{m}$ , covering many basis units in the plane of the substrate. One advantage GLAD has over other fabrication techniques such as self-assembly is the ability to avoid flaws such as dislocations or stacking faults in the crystal lattice that propagate throughout the crystal. However, the structural characteristics of individual spiral arms may vary

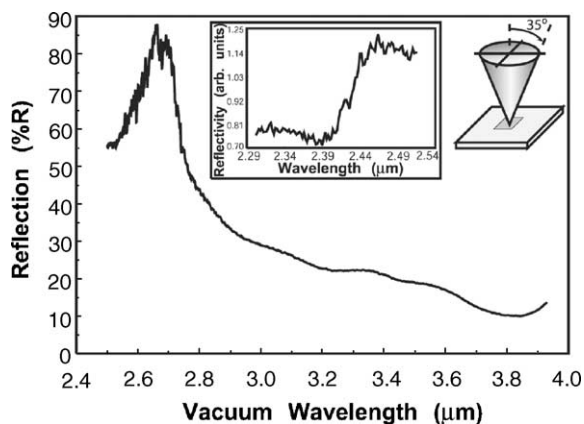


Fig. 2. Reflectance spectra of the photonic crystal for normal incidence with inset showing the shorter wavelength band edge. The band edges for wavevectors normal to the plane of the film show a gap from approximately  $2.44$  to  $2.75 \mu\text{m}$ .

slightly over the surface of a large sample. Due to the local nature of self-shadowing in GLAD films, defects tend to be limited to the scale of a lattice period and extremely large grains of several square millimetres can be fabricated and easily characterized with instruments having a large spot size. Shown in Fig. 2 is the reflection spectrum obtained for normal incidence reflection. As can be seen in the plot, there is a transition at approximately  $2.75 \mu\text{m}$  corresponding to the dielectric band edge and represents the low frequency edge in the  $\Gamma$ -Z-direction of the established Brillouin zone [6,9].

As the FTIR spectrometer is limited to a lower wavelength of  $2.5 \mu\text{m}$ , a normal incidence reflection spectrum for the higher frequency band edge is shown in the inset of Fig. 2. This measurement was performed using a Perkin-Elmer Lambda 900 spectrophotometer and the optical system had a numerical aperture of approximately 0.60, closely duplicating the longer wavelength measurement. The spectrum shows a transition in the reflectivity at  $2.44 \mu\text{m}$ , giving an approximate value for the high frequency air band edge, again in the direction normal to the substrate. We interpret the reduced plateau width and broad wings of the reflection peak as a consequence of small fluctuations in the spiral arm properties over the  $250 \mu\text{m}$  spot size. The fluctuations lead to local variations of both the PBG and the normal incidence stop gap across the sample. Fig. 3 shows the position of the stop gap edges as cal-

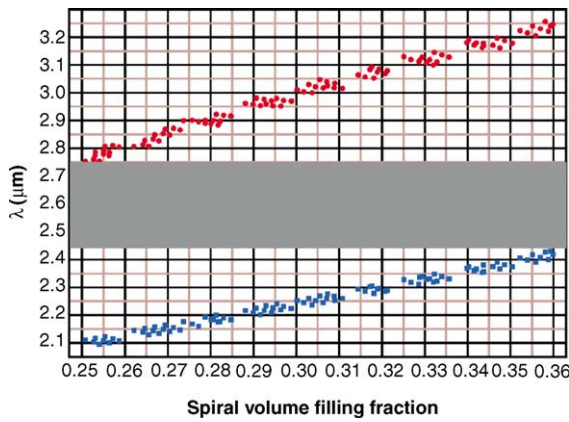


Fig. 3. The edges of the normal incidence stop gap ( $\Gamma$ -Z-direction) as a function of spiral's volume fraction. Each pair of points corresponds to a structure characterized by a dielectric constant of 11.3 and a particular  $[L, c, e]$  uniformly distributed in the 3D parameter space  $\Delta L \times \Delta c \times \Delta e = [0.70, 0.74] \times [1.39, 1.41] \times [0.33, 0.40]$ . The intersection of all the stop gaps is highlighted and extends from 2.45 to 2.75  $\mu\text{m}$ .

culated theoretically for a set of structures with varying spiral arm properties. Each pair of points represents a particular  $[L, c, e]$  uniformly distributed in the 3D volume  $\Delta L \times \Delta c \times \Delta e = [0.70, 0.74] \times [1.39, 1.41] \times [0.33, 0.40]$ , corresponding to variations in the local volume fraction of silicon from 0.25 to 0.36. The intersection of all stop gaps is highlighted and extends from 2.45 to 2.75  $\mu\text{m}$ , matching the observed position and width of the reflectivity plateau.

To test the off-normal band characteristics of our three-dimensional crystal, reflectance measurements were performed using the FTIR spectrometer and a grazing angle reflectance accessory. This measurement is done by an annular beam directed at a central point at angles from  $65^\circ$  to  $85^\circ$  from normal and the result is effectively an average of all measured propagation directions. The resultant peak in the spectrum, as seen in Fig. 4, is a favourable indication of the fact that the crystal has at least some omni-directional characteristics, suggestive of a full photonic band gap. With this experimental configuration, it is possible that averaging of the spectrum over the azimuthal angles has blurred some of the detail of the band structure. The broad wings in the peak are consistent with our picture of variations in the spiral structure across the surface of the deposited film. Moreover, the overlap of this spectrum with the one taken at normal inci-

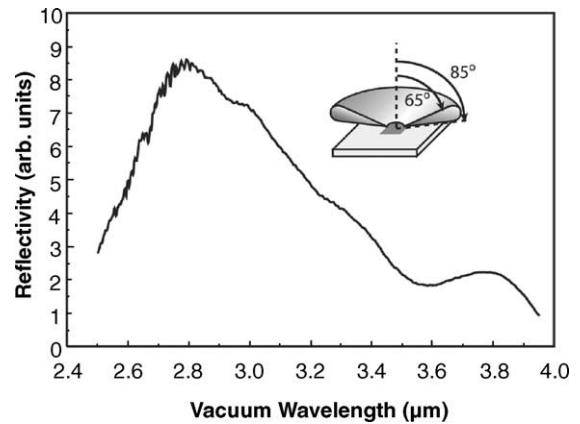


Fig. 4. FTIR reflectance spectra for grazing angle incidence measurements. The non-normal angles of incidence are uniformly distributed about the azimuth of the optics and the result is a superposition of all directions within the annulus. A broad reflectivity peak emerges across the spectrum of interest with the reflectivity peak indicating a band gap from 2.5 to 2.9  $\mu\text{m}$ .

dence is consistent with our interpretation of a local, but full, three-dimensional photonic band gap, which varies slightly in frequency and magnitude from region to region of the structure.

In order to study the nature of the local PBG, in-plane or edge reflection measurements were also performed on a second crystal fabricated with the same parameters as above. An FTIR Bruker IFS-66 fast Fourier transform spectrophotometer with a  $36\times$  Cassegrain objective was used to image a spot size of 12.5  $\mu\text{m}$  on the edge of the cleaved sample. Spectra were obtained by scanning across the edge of the patterned crystal at intervals of 12.5  $\mu\text{m}$ . The results are shown in Fig. 5, where the emergent peak again lies in the range of 2.50–2.75  $\mu\text{m}$  and the frequency and width of the observed reflectivity peak exhibit small (roughly 10%) variations from spot to spot. This is consistent with the local variation in the silicon volume fraction used in our theoretical model to describe the reflectivity from the 250  $\mu\text{m}$  spot. The fact that up to a 10% variation is observed over a 12.5  $\mu\text{m}$  range suggests that the deposited square spiral film exhibits disorder on relatively short length scales and it is likely that the photonic band gap for this sample contains localized states of light rather than being completely devoid of electromagnetic waves. The precision of this instrument also shows the appearance

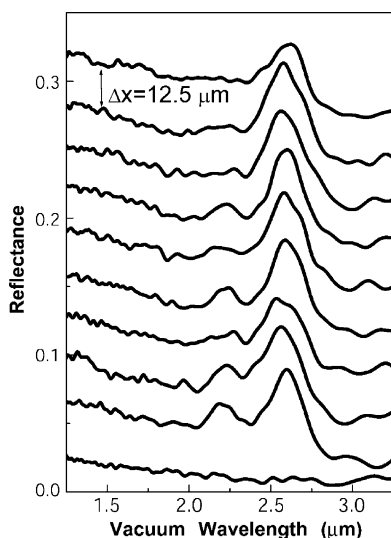


Fig. 5. In plane or edge reflectance measurements taken with a Cassegrain objective and an imaged spot size of  $12.5\ \mu\text{m}$ . The plots represent the measured spectra at different locations on the edge of the sample with each measurement taken at  $12.5\ \mu\text{m}$  intervals. The bottom spectrum was measured on an unpatterned region of the substrate corresponding to random spirals, while the reflectivity peak across the patterned region indicates a band gap from  $2.50$  to  $2.75\ \mu\text{m}$ . The measurements near the bottom indicate the emergence of another stop gap at slightly shorter wavelengths.

at certain locations of a high reflectivity side lobe at higher frequency. As shown in Fig. 6, the bandstructure above the fundamental gap is highly sensitive to the choice of structure parameters describing the spiral posts.

The coincidence of the above measurements suggests the presence of a roughly 10% three-dimensional band gap for IR wavelengths from  $2.50$  to  $2.75\ \mu\text{m}$  over significant regions of the sample. In the theoretical model, it was necessary to consider a statistical distribution of ideal crystals with a PBG in the range of 9–14% and centred in the range of  $2.45$ – $2.9\ \mu\text{m}$ . This statistical distribution can be attributed to minor imperfections of film structure that we expect to overcome with careful development and more stringent control over the deposition conditions such as substrate patterning, temperature, and deposition rate. One other factor affecting the bandwidth and location of the gap that is important when considering actual deposited silicon square spiral structures is the change in the index of refraction due to contamination by oxygen

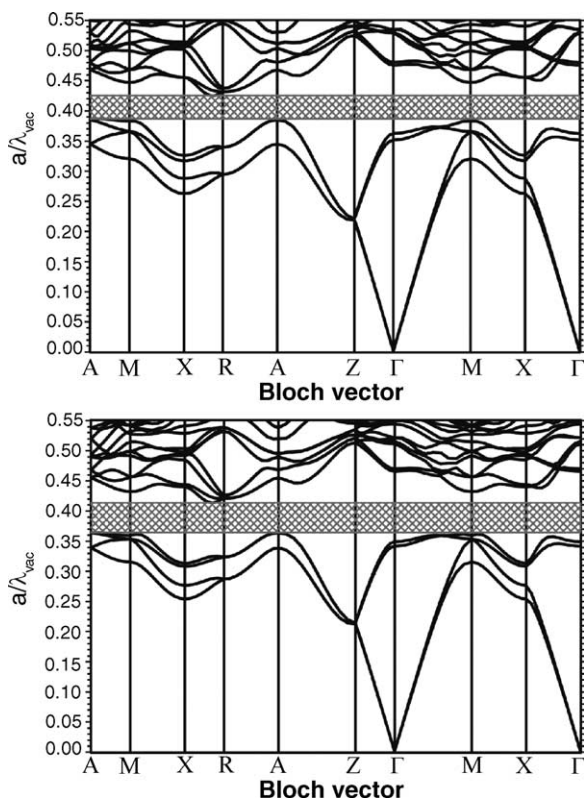


Fig. 6. Two typical photonic band structures for two different geometries of the spirals taken from the statistical distribution of spiral parameters used to fit the optical reflection spectrum of the overall film. Top corresponds to  $[L, c, e] = [0.71, 1.40, 0.33]$  with a 9% PBG and the bottom to  $[L, c, e] = [0.73, 1.39, 0.34]$  with a 12% PBG. The bands above the photonic band gap change significantly with the structural parameters.

and the amorphous nature of the material. From energy dispersive X-ray analysis of the GLAD deposited square spiral photonic crystals, it was found there is contamination by oxygen of approximately 8%, yielding an effective dielectric constant of  $\varepsilon = 11.3$  [14]. This corresponding decrease in the index of refraction has the effect of reducing the bandwidth of the gap while pushing it to shorter wavelengths. The wavelength dependence of the crystal in the IR spectrum is a result of the structure dimensions and lattice spacing. Because of the linearity of Maxwell's equations along with the scalability of the GLAD process, in the future it should be readily possible to scale the centre frequency of the band gap to the NIR or visible range.

## Acknowledgements

Supported by the Natural Science and Engineering Research Council of Canada (NSERC), the Alberta Informatics Circle of Research Excellence (iCORE), the Alberta Ingenuity Fund and Micralyne, Inc. We also acknowledge the assistance of G. Braybrook in his SEM imaging.

## References

- [1] S. John, Strong localization of photons in certain disordered dielectric superlattices, *Phys. Rev. Lett.* 58 (1987) 2486–2489.
- [2] E. Yablonovitch, Inhibited spontaneous emission in solid-state physics and electronics, *Phys. Rev. Lett.* 58 (1987) 2059–2062.
- [3] A. Blanco, E. Chomski, S. Grachtchak, M. Ibsate, S. John, S.W. Leonard, C. Lopez, F. Meseguer, H. Miguez, J.P. Mondia, G.A. Ozin, O. Toader, H.M. van Driel, Large-scale synthesis of a silicon photonic crystal with a complete three-dimensional band gap near 1.5  $\mu\text{m}$ , *Nature* 405 (2000) 437–440.
- [4] C.C. Cheng, A. Scherer, Fabrication of photonic band-gap crystals, *J. Vac. Sci. Technol. B* 13 (1995) 2696–2700.
- [5] H.S. Sozuer, J.P. Dowling, Photonic band calculations for woodpile structures, *J. Mod. Opt.* 41 (1994) 231–239.
- [6] O. Toader, S. John, Proposed square spiral microfabrication for large three-dimensional photonic band gap crystals, *Science* 292 (2001) 1133–1135.
- [7] A. Chutinan, S. Noda, Spiral three-dimensional photonic-band-gap structure, *Phys. Rev. B* 57 (1998) R2006–R2008.
- [8] S.R. Kennedy, M.J. Brett, O. Toader, S. John, Fabrication of tetragonal square spiral photonic crystals, *Nano Lett.* 2 (2002) 59–62.
- [9] O. Toader, S. John, Square spiral photonic crystals: robust architecture for microfabrication of materials with large three-dimensional photonic band gaps, *Phys. Rev. E* 66 (2002) 016610.
- [10] A. Chutinan, O. Toader, S. John, Diffractionless flow of light in all-optical microchips, *Phys. Rev. Lett.* 90 (2003) 123901.
- [11] K. Robbie, L.J. Friedrich, S.K. Dew, T. Smy, M.J. Brett, Fabrication of thin-films with highly porous microstructures, *J. Vac. Sci. Technol. A* 13 (1995) 1032–1035.
- [12] K. Robbie, J.C. Sit, M.J. Brett, Advanced techniques for glancing angle deposition, *J. Vac. Sci. Technol. B* 16 (1998) 1115–1122.
- [13] K. Robbie, M.J. Brett, Method of depositing shadow sculpted thin films, US Patent No. 5,866,204 (1999).
- [14] R. Jacobsen, in: G. Hass, M. Francombe, R. Hoffman (Eds.), *Inhomogeneous and Coevaporated Homogeneous Films for Optical Applications*, *Phys. Thin Films* 8 (1975) 51–98.